

An x-ray probe of laser-aligned molecules

Emily R. Peterson,* Christian Buth, Dohn A. Arms, Robert W. Dunford, Elliot P. Kanter, Bertold Krässig, Eric C. Landahl, Stephen T. Pratt, Robin Santra, Stephen H. Southworth, and Linda Young
Argonne National Laboratory, Argonne, Illinois 60439, USA

(Dated: 07 March 2008)

We demonstrate a hard x-ray probe of laser-aligned small molecules. To align small molecules with optical lasers, high intensities at nonresonant wavelengths are necessary. We use 95 ps pulses focused to $40\ \mu\text{m}$ from an 800 nm Ti:sapphire laser at a peak intensity of $10^{12}\ \text{W}/\text{cm}^2$ to create an ensemble of aligned bromotrifluoromethane (CF_3Br) molecules. Linearly polarized, 120 ps x-ray pulses, focused to $10\ \mu\text{m}$, tuned to the Br $1s \rightarrow \sigma^*$ pre-edge resonance at 13.476 keV, probe the ensemble of laser-aligned molecules. The demonstrated methodology has a variety of applications and can enable ultrafast imaging of laser-controlled molecular motions with Ångstrom-level resolution.

PACS numbers: 32.80.Lg, 32.30.Rj

Intense laser fields have greatly expanded our ability to control the behavior of isolated atoms and molecules.^{1,2} A nonresonant, linearly polarized laser field will align a molecule by interaction with the molecule's anisotropic polarizability; the most polarizable axis within the molecule will align parallel to the laser polarization axis.³ Since the laser polarization direction is under simple control with a waveplate, so is the direction of the molecule's most polarizable axis with respect to the laboratory frame. The polarizability interaction used to align molecules is identical to that used in optical trap^{4,5} studies of biomolecules, though the alignment aspect is not usually emphasized.⁶ Such experiments routinely use visible light probes and achieve nanometer-level resolution.⁶ Here we demonstrate the use of 0.9 Å x-rays to probe a transient ensemble of laser-aligned molecules, thus, taking a step toward Ångstrom-level ultrafast imaging of molecular motions.

Laser control of molecular alignment enables control over x-ray processes. For instance, scattering from an ensemble of aligned molecules produces Bragg-like diffraction spots rather than the concentric rings observed in scattering from an isotropic gas. An important application is biomolecule structure determination with few Ångstrom resolution using coherent diffractive imaging with hard x-ray free-electron lasers.⁷ The original concept⁷ did not suggest aligned molecules but rather proposed to scatter 10^{12} x-rays from a single biomolecule within 10 fs and collect a diffraction pattern with sufficient information to determine the molecule's orientation in a single shot. A recent experiment using the FLASH free-electron laser operating at 320 Å provides an important proof of principle.⁸ As an alternative, having prealigned molecules will vastly simplify the data collection and analysis.⁹ While both proposals^{7,9} focus on x-ray scattering from a *single* large molecule and multiple repetition to build up statistics, i.e., “serial crystallography,” our work focuses on x-ray probing of an *ensemble* of 10^7 small molecules in the gas phase which have been aligned with laser techniques.² This strategy will allow one to acquire x-ray diffraction patterns of aligned, non-interacting molecules and, thus, obtain Ångstrom-level

molecular images using existing synchrotron sources.

To demonstrate the essential ideas, we focus here on the simpler situation of resonant x-ray absorption to probe laser-aligned molecules. X-ray absorption resonances, resulting from the promotion of a $1s$ electron (localized on a given atom) to an empty σ^* or π^* orbital (fixed to the molecular frame), are sensitive to the relative angle between the molecular axis and the x-ray polarization axis.¹⁰ We studied the nonhazardous, symmetric top molecule bromotrifluoromethane (CF_3Br). Using *ab initio* methods, we calculate that the C–Br axis is the most polarizable and will align parallel to the laser polarization axis. The CF_3Br alignment axis can be rotated with respect to the x-ray polarization axis and a linear dichroism indicative of the degree of molecular alignment results. For CF_3Br , the Br $1s \rightarrow \sigma^*$ pre-edge resonance is an excitation from the Br $1s$ orbital to an antibonding σ^* orbital containing substantial Br $4p_z$ character, where z refers to the C–Br axis. As a result of the molecular symmetry, x-ray absorption on the Br $1s \rightarrow \sigma^*$ resonance occurs only when the x-ray polarization vector has a non-vanishing projection on the C–Br axis.

Two basic experiments demonstrate the x-ray probe of laser-aligned molecules. First, we show that resonant x-ray absorption changes reversibly in the presence of the laser field by measuring a laser/x-ray cross correlation. The ensemble is aligned only transiently and a theory including time dependence is required to describe the dynamics of molecular alignment.¹¹ Second, we demonstrate control of x-ray absorption on the Br $1s \rightarrow \sigma^*$ resonance by rotating the alignment of CF_3Br molecules with respect to the x-ray polarization axis. For each of these experiments, we compare with a theory developed to describe x-ray absorption of laser-aligned molecules.¹²

Our experimental arrangement (Fig. 1) used micro-focused x-rays to probe rotationally cooled CF_3Br in the presence of the linearly polarized aligning laser field. A $\lambda/2$ waveplate controlled ϑ_{LX} , the angle between the x-ray and laser polarization axes. Monochromatic, linearly polarized x-rays near 13.5 keV [bandwidth is 0.7 eV full width at half maximum (FWHM)] from an undulator source at Sector 7 of the Advanced Photon

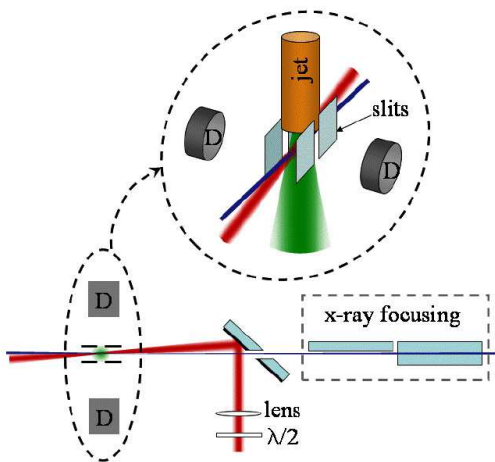


FIG. 1: (Color online) Schematic of experimental setup, top view. Inset with projection of interaction region: jet, collimation slit geometry and Si drift detectors (D).

Source were focused to $10\ \mu\text{m}$ (FWHM) and overlapped collinearly with the $40\ \mu\text{m}$ (FWHM) aligning laser beam. Ti:sapphire oscillator pulses were stretched and amplified to produce alignment pulses (1.9 mJ, 95 ps FWHM) at a repetition rate of 1 kHz. The four dimensional overlap (temporal and spatial) was done with methods previously described.¹³ The signature of CF_3Br x-ray absorption, Br $K\alpha$ fluorescence at 11.9 keV, was viewed with Si drift detectors through molybdenum slits that limited the detection to the central 1.2 mm of the laser/x-ray overlap region. Spatial averaging over the crossing angle and viewed region yielded a peak laser intensity of $(0.85 \pm 0.09) \times 10^{12}\ \text{W}/\text{cm}^2$. CF_3Br was rotationally cooled by expanding a mixture of 10% CF_3Br /90% helium through pinhole nozzles of diameter $d = 25$ or $50\ \mu\text{m}$ at backing pressures up to $P_0 = 9$ bar. The laser and x-ray beams intersected the supersonic expansion ~ 1 mm downstream of the nozzle, where the number density of CF_3Br was $\sim 5 \times 10^{14}/\text{cm}^3$.

The x-ray absorption spectrum of CF_3Br shown in Fig. 2 was obtained by collecting Br $K\alpha$ fluorescence as a function of the incident x-ray energy. The Br $1s \rightarrow \sigma^*$ resonance at 13.476 keV is the prominent feature below the Br K -edge energy. The resonance was fit to a Lorentzian with $\Gamma = 2.6$ eV and the Br K -edge plus Rydberg excitations were fit to an arctangent function.¹⁴ The arctangent function contributes a 10% background under the Br $1s \rightarrow \sigma^*$ resonance.

In the first experiment, we measured a laser/x-ray cross-correlation signal by tuning the x-ray energy to the Br $1s \rightarrow \sigma^*$ resonance and varying the laser/x-ray time delay τ . Figure 3(a) shows the cross-correlation signal, defined by the ratio of parallel ($\vartheta_{\text{LX}} = 0^\circ$) to perpendicular ($\vartheta_{\text{LX}} = 90^\circ$) x-ray absorption, as a function of laser/x-ray delay. The ratio was formed after subtracting the 10% background discussed above. The alignment evolves adiabatically—following the laser pulse envelope.

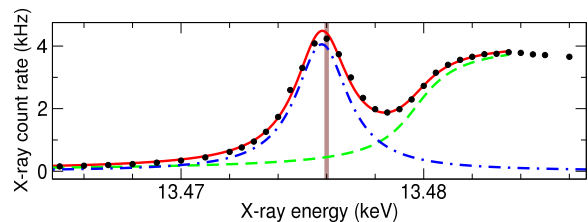


FIG. 2: (Color online) X-ray absorption spectrum of CF_3Br near the Br K edge. Experimental data (dots). The Br $1s \rightarrow \sigma^*$ resonance of CF_3Br at 13.476 keV is marked with a vertical line. The fitted components and their sum are shown: Br $1s \rightarrow \sigma^*$ resonance (dash-dot), Br K edge (dashed), and sum (solid).

A Gaussian fit to the cross correlation signal yields a FWHM of 150 ± 14 ps and amplitude of 1.22 ± 0.03 . We calculated for comparison with experiment the absorption cross sections for (1) parallel laser and x-ray polarizations, (2) perpendicular laser and x-ray polarizations, and (3) a laser-free thermal ensemble.¹² In these calculations, the only adjustable parameters are the rotational temperature and the pulse length of the x-rays. The relevant molecular parameters, e.g., rotational constants, calculated by theory are in agreement with measured values. Comparison of the cross-correlation signal with theory yields an x-ray pulse length of 122 ± 18 ps, consistent with expectations.

The usual criterion for adiabatic molecular response is $\tau_{\text{pulse}} \gg \tau_{\text{rot}}$, where τ_{pulse} is the laser pulse duration and τ_{rot} is the rotational period of the molecule.² A 20 K thermal ensemble of CF_3Br has an average rotational period of 28 ps, much less than our 95 ps laser pulse duration, thus, fulfilling the adiabatic criterion (the ground state rotational period of CF_3Br is 235 ps for rotation about an axis perpendicular to the C–Br axis¹⁵). The commonly used measure of molecular alignment is $\langle \cos^2 \theta \rangle$, where θ is the angle between the laser polarization and the molecular axis. For our experimental parameters, we calculated that the evolution of $\langle \cos^2 \theta \rangle$ follows the laser pulse envelope, as shown in Fig. 3(b).

After optimizing temporal overlap at $\tau = 0$, we demonstrate control of resonant x-ray absorption by varying the angle between the laser and x-ray polarizations, ϑ_{LX} (Fig. 4). The quantity plotted on the ordinate is the ratio of the Br $K\alpha$ fluorescence signal from the aligned sample (laser on) to the isotropic sample (laser off). A maximum occurs for the parallel configuration $\vartheta_{\text{LX}} = 0^\circ$ and a minimum for the perpendicular configuration $\vartheta_{\text{LX}} = 90^\circ$. This confirms the symmetry of the σ^* resonance with respect to the C–Br axis. To compare with experiment, we calculated the ϑ_{LX} dependence of the laser-on/laser-off ratio at $\tau = 0$, as shown in Fig. 4 where good agreement is found for a rotational temperature $T_{\text{rot}} = 24 \pm 2$ K and x-ray pulse duration of 122 ps, determined from the cross-correlation measurement.

Significant improvement in the degree of alignment can be achieved with lower rotational temperature or higher

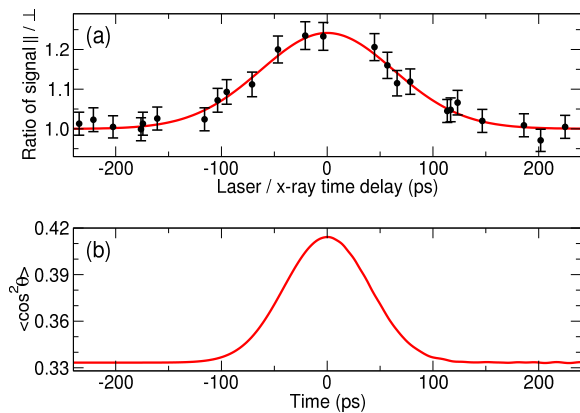


FIG. 3: (Color online) (a) Laser/x-ray cross correlation for laser-aligned CF_3Br , \parallel / \perp absorption as a function of laser/x-ray delay. Theory for a rotational temperature $T_{\text{rot}} = 20$ K is overlaid. (b) Calculated $\langle \cos^2 \theta \rangle$ for a 95 ps (FWHM) laser pulse with an intensity of 0.85×10^{12} W/cm 2 for $T_{\text{rot}} = 20$ K.

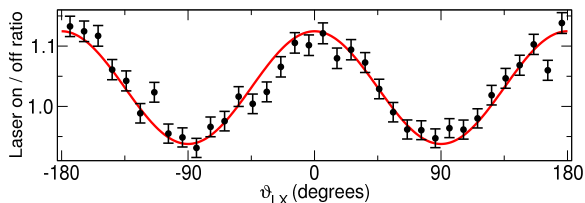


FIG. 4: (Color online) Laser on/laser off ratio of Br fluorescence induced by x-ray excitation on the Br $1s \rightarrow \sigma^*$ resonance of CF_3Br at 13.476 keV, as a function of ϑ_{LX} . $\vartheta_{\text{LX}} = 0^\circ$ and 90° correspond to the parallel and perpendicular configurations for laser and x-ray polarizations. Theory for $T_{\text{rot}} = 24$ K is the overlaid curve.

laser alignment intensity. At 20 K, we observed a linear dependence of the alignment up to our maximum peak intensity of $\sim 10^{12}$ W/cm 2 with no ionization. Our expansion provided significantly less rotational cooling than a pulsed expansion ($P_0 = 100$ bar, $d = 200$ μm) where rotational temperatures ~ 1.5 K have been obtained.¹⁶ Our calculations for 1 K predict the alignment magnitude to increase to $\langle \cos^2 \theta \rangle = 0.80$ and the alignment duration to 140 ps (FWHM) for $\tau_{\text{pulse}} = 95$ ps.

The present work suggests several applications using x-ray absorption. First, polarized x-ray absorption by molecules whose axes are aligned in space enables the assignment of the symmetries (e.g., σ^* and π^*) of near

edge resonances. These techniques have been used for molecules adsorbed on surfaces,¹⁰ but they can now be extended generally to isolated molecules in the gas phase. They are more general than angle-resolved photoion yield spectroscopic methods¹⁷ which rely on ion dissociation and the axial recoil approximation. In addition, x-rays are ideal probes of laser-aligned molecules in the solution phase, where Coulomb explosion imaging techniques typically used in gas phase experiments^{2,16} are not applicable. An x-ray probe is also free from the complications of strong-field probes arising from complex ionization pathways.¹⁸ There also is an opportunity to use x-rays as a probe of laser-controlled rotations to achieve a better understanding of solvent dynamics.¹⁹ The penetrating power of x-rays in low- Z solvents, combined with the localized core-level absorption on the solute molecule, are both significant assets. The advent of tunable, polarized 1 ps x-rays at the Advanced Photon Source²⁰ will enable tracking rotational dynamics in condensed phases as well as impulsively aligned molecules in the gas phase.

Finally, our work demonstrates column densities of aligned molecules that are sufficient for coherent diffraction imaging. We already have achieved an aligned molecule density of $\sim 5 \times 10^{14}$ /cm 3 , corresponding to 4×10^7 molecules within the laser/x-ray overlap volume. With this density, we estimate that less than 6 min is required to acquire a coherent diffraction image for the prototypical Br_2 with a total of 10^5 events, assuming an elastic scattering cross section of 1.6 kb (obtained by summing the contributions of the individual atoms), 10^8 x-rays/pulse/(10 μm) 2 at a repetition rate of 1 kHz. At a 10% seeding fraction, the coexpanded He would provide only a $\sim 2\%$ background and dimer formation is expected to be $< 1\%$. Thus, this demonstration can be considered a first step toward Ångstrom-level x-ray imaging of uncrystallized molecules.

Acknowledgments

This work and the Advanced Photon Source were supported by the Chemical Sciences, Geosciences, and Biosciences Division of the Office of Basic Energy Sciences, Office of Science, U.S. Department of Energy, under Contract No. DE-AC02-06CH11357. C.B. was partly supported by a Feodor Lynen Research Fellowship from the Alexander von Humboldt Foundation.

* Present address: University of Michigan, Ann Arbor, Michigan 48109, USA

¹ K. Yamanouchi, *Science* **295**, 1659 (2001).

² H. Stapelfeldt and T. Seideman, *Rev. Mod. Phys.* **75**, 543 (2003).

³ B. Friedrich and D. Herschbach, *Phys. Rev. Lett.* **74**, 4623 (1995).

⁴ A. Ashkin, *Phys. Rev. Lett.* **24**, 156 (1970).

⁵ A. Ashkin, *Appl. Phys. Lett.* **19**, 283 (1971).

⁶ K. C. Neuman and S. M. Block, *Rev. Sci. Instrum.* **75**, 2787 (2004).

⁷ R. Neutze, R. Wouts, D. van der Spoel, E. Weckert, and J. Hajdu, *Nature* **406**, 752 (2000).

⁸ H. N. Chapman, A. Barty, M. J. Bogan, S. Boutet,

- M. Frank, S. P. Hau-Riege, S. Marchesini, B. W. Woods, S. Bajt, W. Benner, R. A. London, E. Plönjes, M. Kuhlmann, R. Treusch, S. Düsterer, T. Tschentscher, J. R. Schneider, E. Spiller, T. Möller, C. Bostedt, M. Hoener, D. A. Shapiro, K. O. Hodgson, D. van der Spoel, F. Burmeister, M. Bergh, C. Caleman, G. Hultdt, M. M. Seibert, F. R. N. C. Maia, R. W. Lee, A. Szöke, N. Timneanu, and J. Hajdu, *Nat. Phys.* **2**, 839 (2006).
- ⁹ J. C. H. Spence and R. B. Doak, *Phys. Rev. Lett.* **92**, 198102 (2004).
- ¹⁰ J. Stöhr, *NEXAFS Spectroscopy* (Springer, New York, 1996).
- ¹¹ R. Torres, R. de Nalda, and J. P. Marangos, *Phys. Rev. A* **72**, 023420 (2005).
- ¹² C. Buth and R. Santra, *Phys. Rev. A* **77**, 013413 (2008).
- ¹³ L. Young, D. A. Arms, E. M. Dufresne, R. W. Dunford, D. L. Ederer, C. Höhr, E. P. Kanter, B. Krässig, E. C. Landahl, E. R. Peterson, J. Rudati, R. Santra, and S. H. Southworth, *Phys. Rev. Lett.* **97**, 083601 (2006).
- ¹⁴ B. K. Agrawal, *X-ray Spectroscopy* (Springer, Berlin Heidelberg, 1991).
- ¹⁵ A. P. Cox, G. Duxbury, J. A. Hardy, and Y. Kawashima, *J. Chem. Soc., Faraday Trans. 2* **76**, 339 (1980).
- ¹⁶ V. Kumarappan, C. Z. Bisgaard, S. S. Viftrup, L. Holmegaard, and H. Stapelfeldt, *J. Chem. Phys.* **125**, 194309 (2006).
- ¹⁷ J. Adachi, N. Kosugi, and A. Yagishita, *J. Phys. B.* **38**, R127 (2005).
- ¹⁸ D. Pavičić, K. F. Lee, D. M. Raymer, P. B. Corkum, and D. M. Villeneuve, *Phys. Rev. Lett.* **98**, 243001 (2007).
- ¹⁹ S. Ramakrishna and T. Seideman, *Phys. Rev. Lett.* **95**, 113001 (2005).
- ²⁰ M. Borland, *Phys. Rev. ST Accel. Beams* **8**, 074001 (2005).